Marine Pollution Bulletin 201 (2024) 116254



Contents lists available at ScienceDirect

Marine Pollution Bulletin

journal homepage: www.elsevier.com/locate/marpolbul





# Numerical and experimental simulation on efficiency of air bubble barrier on various pollutants for preventing oil spill spread

Canberk HAZAR [a,b,*], Ali Cemal TÖZ [c]

[a] Dokuz Eylul University, The Graduate School of Natural and Applied Sciences, Izmir, Türkiye
[b] Zonguldak Bulent Ecevit University, Maritime Faculty, Zonguldak, Türkiye
[c] Dokuz Eylul University, Maritime Faculty, Izmir, Türkiye

ARTICLE INFO

*Keywords:*
Air bubble barrier
Oil spill spread
Numerical simulation
Oil containment barriers
Experimental setup

ABSTRACT

This study conducts experimental and numerical simulations and analyzes the effects of the air bubble barrier (ABB) on the oil spill spread prevention efficiency regarding the varying aperture diameter, air discharge, and pollutant type. In a computational fluid dynamics simulation, a multiphase flow is studied using the finite volume method with the volume of fluid technique in the Star CCM+ software. The pipe generating air bubbles is fixed at the bottom of the tank at 1.8 m from the side of the experimental setup. The distinctive points of the study are the experiments conducted on different pollutants and the utilization of a novel adjustable air nozzle positioned on the air feed pipe. The effectiveness of the ABB in mitigating the spread of marine pollution is contingent on the aperture size, air discharge, and pollutant type. This study demonstrates that the ABB's feasibility for preventing the oil spill spread has improved.

## 1. Introduction

The rapid global economic growth has caused a significant increase in the demand for oil worldwide. This has led to a rise in the oil trade and, subsequently, a notable expansion of the maritime oil transportation industry. Unfortunately, this growth has also resulted in ongoing contamination of the marine environment (Chen et al., 2019). The main causes of these spills include aging infrastructure, dangerous sea conditions, conflict, and activities associated with oil drilling, transportation, shipping, and refining. However, most of these incidents are attributed to pipeline failure, spills from ships, and abandoned refinery sites (Feng and Zhang, 2023). Approximately 15,000 tons of oil were released into the environment because of tanker accidents in 2022. A total of 14,000 tons of oil were discharged during three significant occurrences. Additionally, the spill projections for 2022 rank as the second highest in prior years, according to ITOPF (2022).

Marine spills pose the greatest challenges for response efforts (Talimi et al., 2020). Hence, it is imperative to develop effective methods to combat significant oil spills in the ocean and confine spilled oil to ports and water channels (Kobus, 1975). The effectiveness of the traditional oil containment boom in an oil pollution response process is quite low. In addition, the costs of existing traditional oil containment booms are high, and the emergency response performance required to prevent the spread of oil pollution is poor. It is anticipated that using ABB instead of traditional oil containment booms during an oil pollution response process would save time, reduce costs, and be a more effective solution (Zdrazil, 2022). A pneumatic barrier, sometimes referred to as a bubble curtain or air curtain, can be employed as an alternate approach to managing oil spills (Abraham et al., 1973). A pneumatic oil barrier or air bubble barrier is a system used for waterways or port facilities. It creates a barrier to anything floating in the water, especially floating oil, and shipwrecks. The features that distinguish the air bubble barrier from traditional oil containment booms are that it does not require manpower in its operation, is time-efficient, requires almost no maintenance, has a long operational life, and can be operated even in the event of a fire (Hazar and Töz, 2023a). The pneumatic oil barrier generates a rapid flow over the surface of the water, thereby preventing the oil from spreading beyond it. Ascending air bubbles are what cause the flow, which causes an upward water current. Upon reaching the water's surface, the vertical stream of bubbles divides into two horizontal currents that move away from the original stream (Hydrotechnik Lubeck, 2011). Once equilibrium is established, the current generated by the bubble effectively confines the oil. The pneumatic barrier for containing oil is constructed based on this foundation (Basco, 1971). Typically, the

* Corresponding author at: Dokuz Eylul University, The Graduate School of Natural and Applied Sciences, Izmir, Türkiye.
*E-mail addresses:* canberk.hazar@beun.edu.tr (C. HAZAR), ali.toz@deu.edu.tr (A.C. TÖZ).

https://doi.org/10.1016/j.marpolbul.2024.116254
Received 6 December 2023; Received in revised form 29 January 2024; Accepted 8 March 2024
Available online 14 March 2024
0025-326X/© 2024 Elsevier Ltd. All rights reserved.

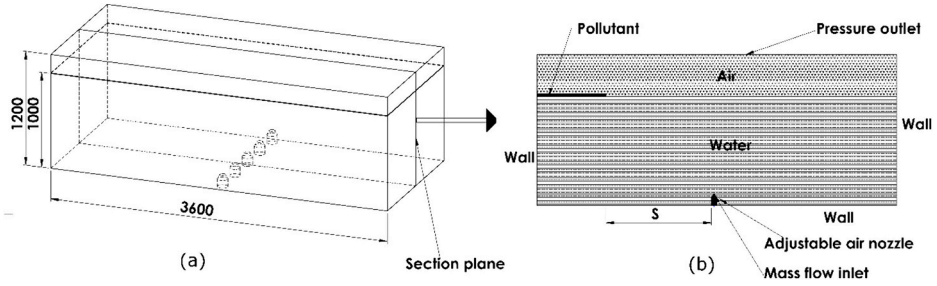


**Fig. 1.** The numerical model for the ABB (a) and boundary conditions of the numerical model (b).

ABBs are fully immersed. Compared to traditional oil booms used on the water surface, the ABB is less affected by natural elements such as wind and waves. Additionally, it does not usually obstruct ship navigation while in use (Lu et al., 2015).

ABBs have found application in various contexts, such as preventing ice formation (Ince, 1964; Cui et al., 2021), enhancing the wave-dissipating capabilities of pneumatic breakwaters (Wang et al., 2019; Zang and Bai, 2012; Zang, 2013; Zdrazil, 2022), serving as barriers to block saltwater intrusion in locks (Abraham and Buirgh, 1964); Simmons, 1967), containing oil spills (Grace and Sowyrda, 1970; Jones, 1972; Lau and Engel, 1980; Delvigne, 1984; Lo, 1997; Fujita, 2016; Eidnes et al., 2013), deterring fish from entering restricted zones (Leander et al., 2021; Ditmars and Cederwall, 1974; Flammang et al., 2014; Welton et al., 2002; Zielinski and Sorensen, 2016), safeguarding finfish pens from unwanted jellyfish (Haberlin et al., 2021; Handå et al., 2013; Zielinski et al., 2014), reducing noise generated during offshore pile driving (Lucke et al., 2011; Tsouvalas and Metrikine, 2016), use as highly effective anti-fouling systems in dredging engineering (Cheng et al., 2021), use on tender platforms set up on the cruises (Bamdadinejad et al., 2020), and use as an air lubrication system to reduce ship navigation resistance (Kim et al., 2020; Kim et al., 2021; Lube et al., 2019; Park and Lee, 2018). Although the ABB has undergone extensive examination for several applications, its main use has been focused on oil pollution containment and wave dissipation. Even though there has been a lot of theoretical and experimental research, we still don't fully understand how water and air bubbles interact in the ABB. This shows how important empirical data is for putting theories into practice. The primary focus of research on the efficiency of the ABB has been on factors such as air discharge, aperture size, and spatial organization of the aperture interval. Research indicates that there are conflicting perspectives regarding the efficacy of the ABB in mitigating marine pollution (Hazar and Töz, 2022).

Lu et al. (2015) conducted numerical calculations and practical experiments to evaluate the effectiveness of the ABB in confining oil in the presence of running water. Their research showed that factors like aperture size, gap between apertures, air pipe submerged depth, number of air pipes used, air discharge rate, and flow characteristics of the surrounding environment have a significant impact on the effectiveness of ABB. Eidnes et al. (2013) conducted experiments and investigations to evaluate the feasibility of using a wide ABB, in the shape of a raft, as a proactive measure in a marine pollution situation. The comprehensive trials carried out at Skarnsundet have demonstrated that enhancing the bubble curtain by transforming it into a bubble raft with the addition of additional parallel pipes has significantly enhanced its efficacy in containing oil spills. This development has rendered it a feasible choice for combating marine pollution. Fujita (2016) specifically focused on the bubble curtain positioned adjacent to a vertical wall, to deploy it to protect land facilities and prevent or remove oil patches that may drift off the pier. The validity of the suggested model is confirmed by comparing it to both numerical simulations and experimental data. There is a discrepancy of 15 % between the experimental and numerical simulations. McClimans et al. (2012) examine the causes of the breakdown of ABB, studying the underlying principles that regulate the dynamics and motion of oil bubbles in both bubble curtains and bubble rafts. Field and laboratory testing have demonstrated the favorable potential of employing distributed bubble plumes for full-scale maritime oil barrier applications. This research has been undertaken autonomously and in collaboration with a bubble-oil barrier skirt. The tandem bubble oil barrier was thoroughly analyzed, and comprehensive fluid dynamics data were collected through large-scale experiments conducted in oil-free flumes. In their research summary on oil spill containment, Feng and Zhang (2023) emphasized the applications and mechanisms of bubble curtains. This article thoroughly analyzed the underlying operational principle of bubble curtains in containing oil spills, the complex difficulties faced by current methods, the potential advantages of combining them with traditional oil containment booms, and the significant scientific matters that necessitate additional investigation. The development of next-generation oil containment techniques will prioritize the performance and structural optimization of the improved oil containment barrier with a bubble curtain. This is in response to concerns regarding the inadequate oil containment performance and improper deployment of the existing conventional oil containment boom under complex and variable sea conditions. The results showed that the methodology can demonstrate how well the air bubble barrier is working and provide a basis for its operation to prevent the spread of oil pollution, thereby helping to prevent the spread of major oil spills.

Findings from the literature review show that studies investigating the air bubble barrier for the prevention of oil pollution spread primarily focus on modeling and the potential of the air bubble barrier to prevent oil pollution spread. Numerical modeling studies focus on air feed pipe submerged depth, aperture interval, aperture diameter, and air discharge-based simulations. The studies concentrate on providing air outlet by drilling holes of desired diameters on the air feed pipe. A literature gap has been identified regarding the oil containment performance of the air bubble barrier on different pollutants and changing the aperture diameter over the nozzle by positioning a special adjustable air nozzle on the air feed pipe. The motivation of the study is to make a difference by conducting experiments on different pollutants and changing the aperture diameter by positioning a special adjustable air nozzle on the air feed pipe. Measuring the oil containment performance of the air bubble barrier by conducting experiments on different pollutants can contribute to the literature in terms of oil spill response plans (OSRP) according to which pollutant is spilled into the sea in case of an oil spill. At the same time, it is thought that positioning a special adjustable air nozzle on the air feed pipe and changing the aperture diameter via the nozzle will serve as a reference for future fully automated air bubble barrier studies. This study presents a numerical model and experimental setup to simulate the effectiveness of ABB in containing the spread of oil pollution. Analyses have been performed to evaluate the performance of ABB in preventing the spread of oil pollution. An air aperture is positioned in the bottom and central sections of the numerical model to generate air bubbles. This paper will focus on examining the impact of various aperture diameters, air discharges, and contaminants on the effectiveness of the ABB. The effectiveness of the ABB in containing the oil will be assessed by measuring the horizontal

**Table 1**
Physical features of the fluids in the numerical simulation.

| | Density (kg/m$^3$) | Dynamic viscosity (Pa.s) | Specific heat (J/kg.K) | Thermal conductivity (W/m.K) |
|---|---|---|---|---|
| Water ($H_2O$) | 997.561 | 8.8871E-4 | 4181.72 | 0.620271 |
| Air | 1.18415 | 1.85508E-5 | 1003.62 | 0.0260305 |
| Gasoline ($C_8H_{17}$) | 751 | 5.0272E-4 | 2404.97 | 0.115446 |
| Diesel ($C_{12}H_{23}$) | 810 | 0.00127 | 2093.92 | 0.157 |
| Heavy fuel oil | 991 | 0.17838 | 2000 | 0.125 |

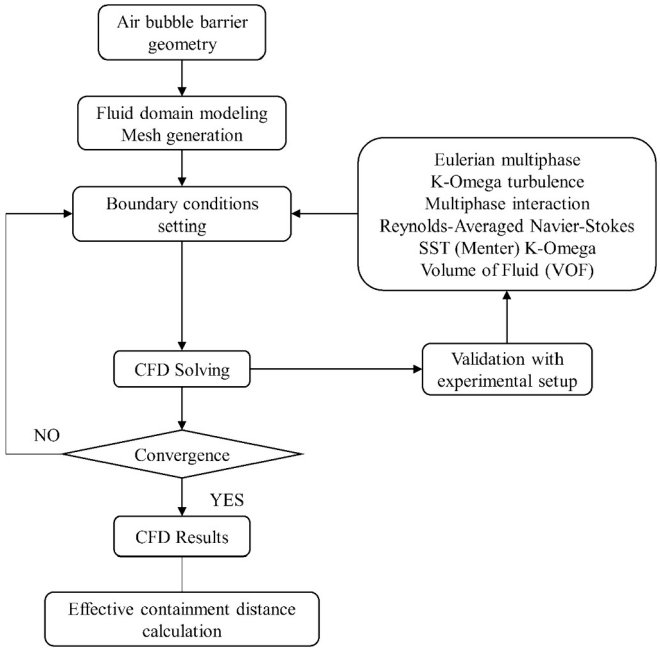


**Fig. 2.** Flowchart of the numerical simulation.

distance between the barrier's position and the front edge of the oil film spread. A higher distance signifies enhanced efficiency (Lu et al., 2015).

The paper is structured as follows. In Section 2, numerical simulation and experimental setup are introduced. In Section 3, the effectiveness of the ABB in blocking the oil spill spread is discussed. Finally, Chapter 4 summarizes the findings of the study, as well as further work to follow.

## 2. Materials and methods

### 2.1. Numerical simulation

In this chapter, we present a mathematical model, boundary conditions, and solution algorithms utilized in the Simcenter STAR CCM+ software. A mathematical model is suggested to simulate the ABB numerically. The numerical model for the ABB and boundary conditions of the numerical model are given in Fig. 1. In this context, a numerical model is employed with dimensions of 3.6 m in length and 1.2 m in depth, while the water depth is maintained at 1 m. The ABB is positioned in the middle and bottom of the numerical model.

The position of the pollutant in the initial state is given in Fig. 1. The effective containment distance (S) refers to the horizontal span between the ABB's location and the leading edge of the oil spill, serving as an indicator of the ABB's efficiency and its ability to contain the oil (Lu et al., 2015).

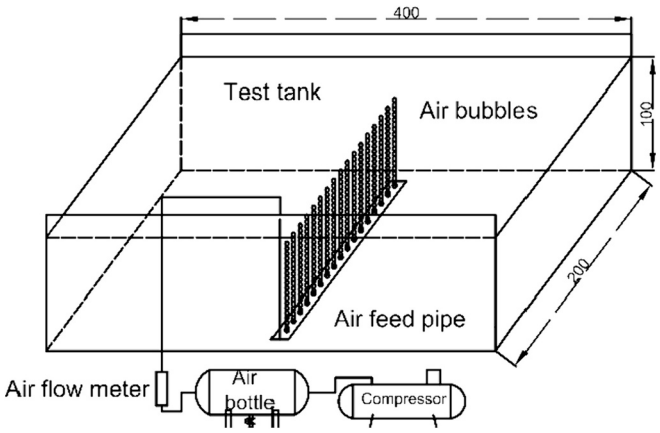


**Fig. 3.** Experimental setup.

The finite volume method within Star CCM+ is employed to solve a multiphase Reynolds Averaged Navier–Stokes (RANS) solver. This solver treats air, water, and pollution as distinct phases and utilizes volume of fluid (VOF) technology. The k–ω shear stress transport (SST) model is used to model turbulence (Xu et al., 2019). The nozzle on the ABB is used as the velocity input. A pressure outlet is used above the calculation area, open to air. A wall boundary condition is applied to both the bottom and sides of the numerical model (Lu et al., 2015). In the initial conditions, there is 1-meter-deep water in the tank. The material properties of water, air, and 3 different types of pollutants are shown in Table 1.

The applied numerical simulation procedure is depicted as a flowchart in Fig. 2. According to the flowchart, at the beginning of the analysis geometry design parameters of the air bubble barrier are defined. For the CFD solver, the fluid domain is modeled with boundary condition settings and mesh is generated. After the CFD solving step, results are validated with an experimental setup. After the validation is completed, CFD results are obtained such as efficient containment distance.

Before the numerical analysis, a mesh convergence study was undertaken to establish the appropriate mesh size and time step size (Hazar and Töz, 2023b). A mesh convergence study was undertaken to identify several elements required in a mathematical model to prove that changing the mesh size does not affect the analysis results. Additional mesh enhancements after convergence did not affect the outcomes of the mesh convergence investigation (Gardiner, 2022).

In the second step of the numerical simulation, the field function is written to locate the pollutant on the water surface. In this simulation, gasoline, diesel, and heavy fuel oil, whose material properties are given in Table 1, are considered pollutants.

### 2.2. Experimental setup

The tests were conducted at the Dokuz Eylul University, Turkey. A schematic of the experimental setup is given in Fig. 3. The tank's dimensions are as follows: it has a length of 4 m, a width of 2 m, and a depth of 1.2 m. The pipe that generates air bubbles is fixed at the tank's bottom, positioned 1.8 m away from one side of the tank. In the experiments, the water depth is set at 1 m.

In this experiment, an adjustable air nozzle has been placed in the air apertures on the pipe. The aperture diameter has been changed by rotating the adjustable air nozzle. The photograph, dimensions, and airflow pattern of the adjustable air nozzle are shown in Fig. 4 (Exair, 2023). The apertures are adjusted to be equal and 10 cm along the pipe. An adjustable air nozzle is placed in the apertures every 10 cm on the pipe. According to Fischer et al. (1979), it is recommended to maintain a gap between the apertures that are smaller than 10 % of the water depth

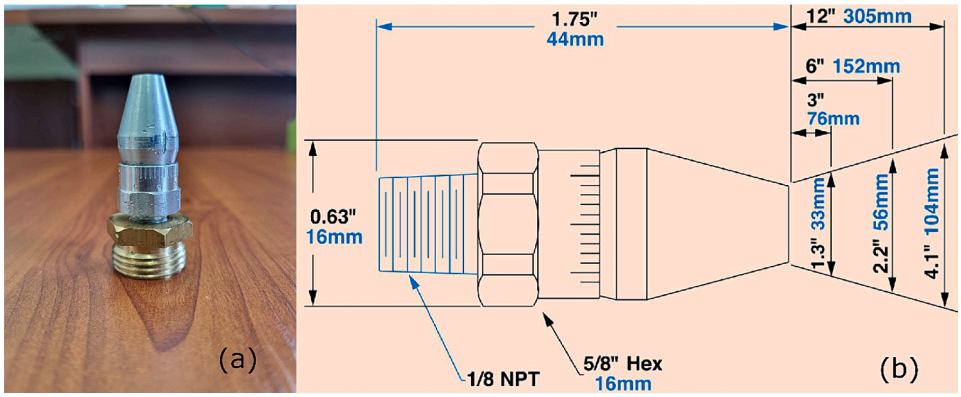


**Fig. 4.** The photograph (a) dimensions, and airflow pattern (b) of the adjustable air nozzle (Exair, 2023).

**Table 2**
The case parameters of the experimental setup.

| Pollutant | Aperture diameter (mm) | Air discharge ($m^3/s$) |
|---|---|---|
| Gasoline, Diesel, Heavy Fuel oil | 1, 1.5, 2 | 0.01, 0.015, 0.02, 0.025, 0.03, 0.035, 0,04 |

to ensure that separate bubble plumes merge before rising to the surface. Air from the compressor is supplied to the submerged air supply pipes after the pressure and volume flow rate are adjusted. The air inside the pipe exits through an adjustable air nozzle on the pipe and a rising column is formed. Upon reaching the water surface, the column alters its flow direction, now moving horizontally outward. This horizontal runoff prevents or removes floating oil particles (Fujita, 2016).

During the experiments, 1.5 l of the pollutant is spilled from one side

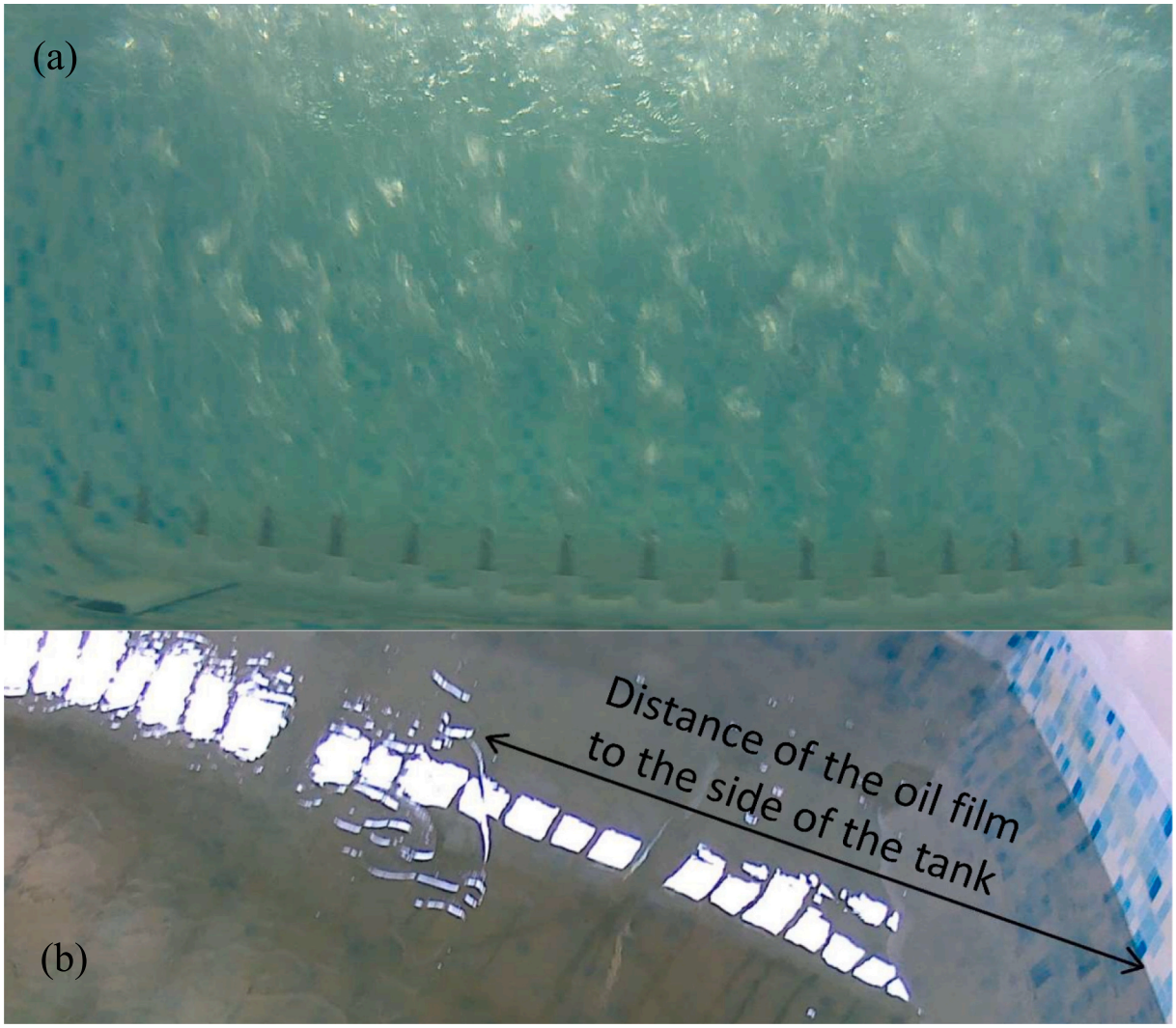


**Fig. 5.** Image of air bubbles in water (a) and image of the water's surface covered in an oil slick (b).

**Table 3**
Classification of typical MAPE values (Moreno et al., 2013).

| MAPE | Interpretation |
|---|---|
| <10 | Highly correct estimation |
| 10–20 | Good estimation |
| 20–50 | Reasonable estimation |
| >50 | Incorrect estimation |

of the test tank, and it is expected to spread over 1 m. After the pollutant spread over 1 m, the system is operated for 5 s, and the efficient containment distance is measured. As carried out in the numerical simulation, to investigate the effects of aperture diameter, air discharge, and different pollutants, different aperture diameters, air discharges, and pollutants will be considered in the experiment. To minimize the potential for measurement errors, each scenario has been executed on a minimum of three separate days. This article presents the measured data's average values. Table 2 displays a compilation of the test conditions that have been established. For the identical scenarios, the outcomes from the numerical analysis are contrasted with the experimental results.

In this study, analyses have been carried out by incrementally raising the air volume flow rate, ranging from 0.01 $m^3/s$ to 0.04 $m^3/s$ in intervals of 0.005 $m^3/s$, and by adjusting the aperture diameter, varying from 1 mm to 2 mm in increments of 0.5 mm, for gasoline, diesel, and heavy fuel oil. Fig. 5(a) shows the special adjustable air nozzles on the air feed pipe in the experimental setup and the air bubbles that form a barrier in the water. Fig. 5(b) shows the oil film formed on the side where the pollutant was poured into the experimental tank and the distance measurement. The calculation of efficient containment distance was made by subtracting the gap between the ABB and the side of the experimental tank from the distance indicated in Fig. 5(b).

In this study, analyses have been carried out based on the limitations given below.

- The physical features of the fluids used in the experimental studies are unknown.
- Numerical model and experimental setup dimensions limit the studies.
- Studies have been conducted with fresh water.
- The experiments have been carried out in summer ambient conditions.
- The experiments have been carried out in quiescent water.

### 2.3. Model verification and validation

The numerical and experimental model is compared using the MAPE score. The mean absolute percentage error quantifies the average magnitude of errors generated by a model. MAPE is identified as the mean absolute percentage error between numerical model data and experimental model data. The MAPE formula is given in Eq. (1) (Wikipedia, 2023).

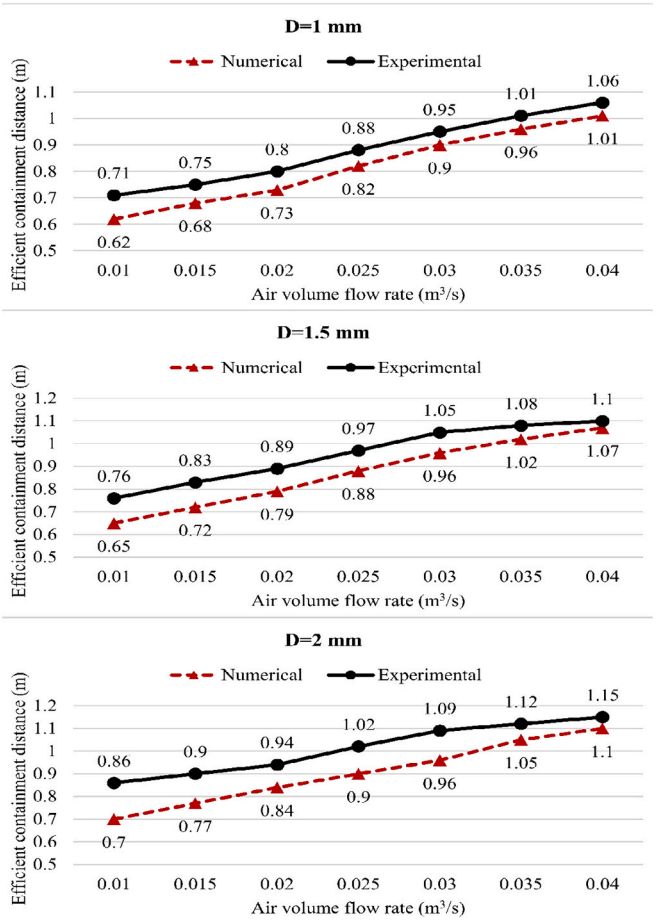


**Fig. 7.** Comparison of the efficient containment distance for gasoline.

$$MAPE = \frac{1}{n}\sum_{t=1}^{n}\left|\frac{A_t - F_t}{A_t}\right| \quad (1)$$

where $A_t$ is the experimental simulation data and $F_t$ is the numerical simulation data. The difference between them is divided by the experimental value $A_t$. For each predicted time point, this ratio's absolute value is added and then divided by the n fitted points. Table 3 provides typical MAPE values for industrial and business data, along with their corresponding explanations.

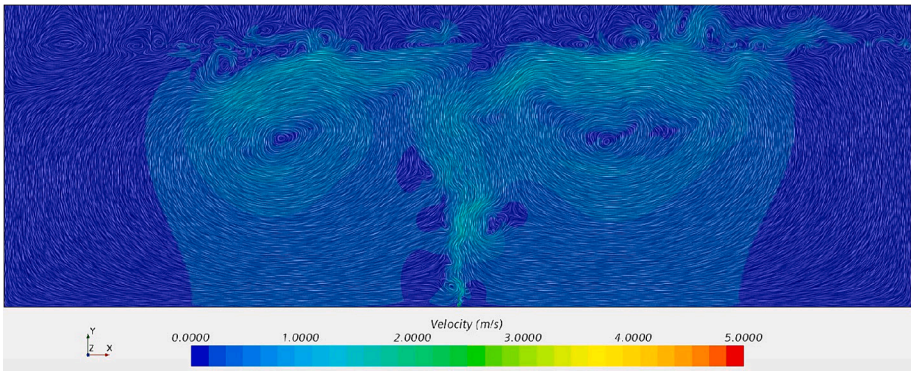


**Fig. 6.** Steady-state velocity field surrounding the ABB and the formation of eddies (numerical simulation, $t$ = 5 s, D = 1.5 mm, and Q = 0.01 $m^3/s$).

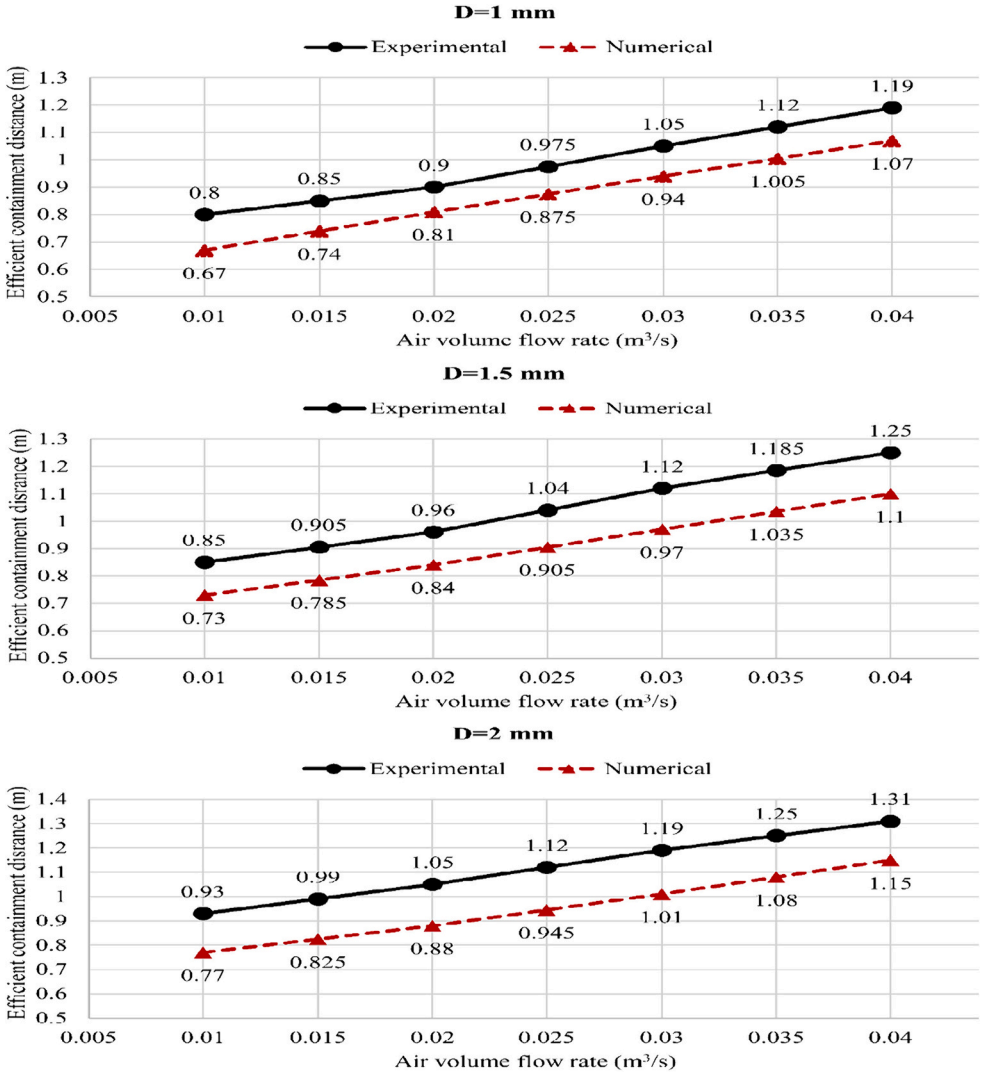


**Fig. 8.** Comparison of the efficient containment distance for diesel.

## 3. Results and discussions

In this study, the numerical model and experimental setup were designed to measure the efficiency of the ABB in blocking oil spills. The study examined how varying the aperture diameter, air discharges, and types of pollutants affected the effectiveness of the ABB. Calculation of the efficient containment distance was figured out by measuring the distance at the end of the 5-second numerical simulation period.

An example showing the velocity distribution and eddies around the ABB is shown in Fig. 6. Because of the buoyancy effects, the air bubbles go higher, causing the water to flow upward. An essential near-surface feature of robust bubble plumes is the conversion of vertical momentum from the upwelling flow into horizontal momentum for the outwelling flow, resulting in the generation of angular momentum. For a 2D plume, this produces a lateral eddy.

Fig. 7 shows the effects of exposure to different aperture diameters and air discharges on the efficiency of the ABB. In such cases, the pollutant type is gasoline, the air volume flow rate is 0.01 $m^3$/s-0.04 $m^3$/s, and the aperture diameter (D) is 1–2 mm. In the numerical simulation, it was observed that as the air discharge from 0.01 $m^3$/s to 0.04 $m^3$/s efficient containment distance increases from 0.62 m to 1.01 m in D = 1 mm, as the air discharge from 0.01 $m^3$/s to 0.04 $m^3$/s efficient containment distance increases from 0.65 m to 1.07 m in D = 1.5 mm, as the air discharge from 0.01 $m^3$/s to 0.04 $m^3$/s efficient containment distance increases from 0.7 m to 1.1 m in D = 2 mm. In the experimental simulation, it was observed that as the air discharge from 0.01 $m^3$/s to 0.04 $m^3$/s efficient containment distance increases from 0.71 m to 1.06 m in D = 1 mm, as the air discharge from 0.01 $m^3$/s to 0.04 $m^3$/s efficient containment distance increases from 0.76 m to 1.1 m in D = 1.5 mm, as the air discharge from 0.01 $m^3$/s to 0.04 $m^3$/s efficient containment distance increases from 0.86 m to 1.15 m in D = 2 mm.

Fig. 8 shows the effects of exposure to different aperture diameters and air discharges on the efficiency of the ABB. In such cases, the pollutant type is diesel, the air volume flow rate is 0.01 $m^3$/s-0.04 $m^3$/s, and the aperture diameter (D) is 1–2 mm. In the numerical simulation, it was observed that as the air discharge from 0.01 $m^3$/s to 0.04 $m^3$/s efficient containment distance increases from 0.67 m to 1.07 m in D = 1 mm, as the air discharge from 0.01 $m^3$/s to 0.04 $m^3$/s efficient containment distance increases from 0.73 m to 1.1 m in D = 1.5 mm, as the air discharge from 0.01 $m^3$/s to 0.04 $m^3$/s efficient containment distance increases from 0.77 m to 1.15 m in D = 2 mm. In the experimental simulation, it was observed that as the air discharge from 0.01 $m^3$/s to 0.04 $m^3$/s efficient containment distance increases from 0.8 m to 1.19 m in D = 1 mm, as the air discharge from 0.01 $m^3$/s to 0.04 $m^3$/s efficient containment distance increases from 0.85 m to 1.25 m in D = 1.5 mm, as the air discharge from 0.01 $m^3$/s to 0.04 $m^3$/s efficient containment distance increases from 0.93 m to 1.31 m in D = 2 mm.

Fig. 9 shows the effects of exposure to different aperture diameters

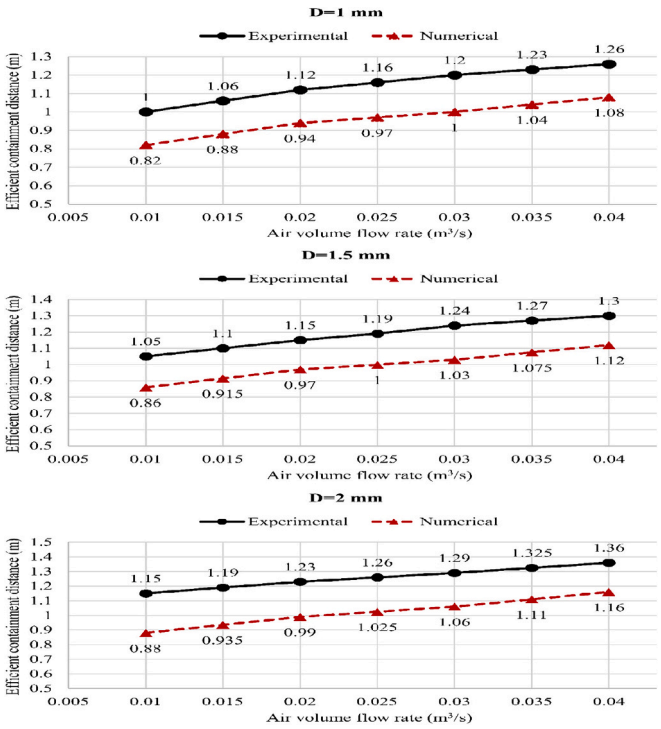


**Fig. 9.** Comparison of the efficient containment distance for heavy fuel oil.

and air discharges on the effectiveness of the ABB. In these cases, the pollutant type is heavy fuel oil, the air volume flow rate is 0.01 $m^3$/s-0.04 $m^3$/s, and the aperture diameter (D) is 1–2 mm. In the numerical simulation, as observed that as the air discharge from 0.01 $m^3$/s to 0.04 $m^3$/s efficient containment distance increases from 0.82 m to 1.08 m in D = 1 mm, as the air discharge from 0.01 $m^3$/s to 0.04 $m^3$/s efficient containment distance increases from 0.86 m to 1.12 m in D = 1.5 mm, as the air discharge from 0.01 $m^3$/s to 0.04 $m^3$/s efficient containment distance increases from 0.88 m to 1.16 m in D = 2 mm. In the experimental simulation, as observed that as the air discharge from 0.01 $m^3$/s to 0.04 $m^3$/s efficient containment distance increases from 1 m to 1.26 m in D = 1 mm, as the air discharge from 0.01 $m^3$/s to 0.04 $m^3$/s efficient containment distance increases from 1.05 m to 1.3 m in D = 1.5 mm, as the air discharge from 0.01 $m^3$/s to 0.04 $m^3$/s efficient containment distance increases from 1.15 m to 1.36 m in D = 2 mm.

As shown in Fig. 7, Fig. 8, and Fig. 9, the efficiency of the ABB increases as the air volume flow rate and aperture diameter increase. At the same time, air volume flow rate has emerged to be a more effective parameter according to aperture diameter in the effectiveness of the ABB. The efficient containment distance of the ABB is higher in case of heavy fuel oil spillage. The results reveal that the dispersion of pollution is related to the viscosity of the pollutant. It has been observed that as the aperture diameter increases, the air bubbles produced become larger, and the frequency of bubble production decreases. Lu et al. (2015) observed in their tests with rapeseed oil that the effective containment distance increased by 19 % when the aperture diameter increased from 1 mm to 2 mm at constant air discharge. In this study, it has been found that under the same conditions, the effective containment distance increased by 21 % in the tests performed with gasoline, 16 % in the tests performed with diesel, and 15 % in the tests conducted with heavy fuel oil. Also, Lu et al. (2015) found in their experiments that when the air discharge doubles at a fixed aperture diameter, the effective containment distance increases by 30 % for 1 mm, 25 % for 1.5 mm, and 17 % for 2 mm. In this study, when the effective containment distance was averaged for 3 pollutants under the same conditions, the aperture diameter was 25 % for 1 mm, 22 % for 1.5 mm, and 19 % for 2 mm. It has been seen that at air discharges higher than 0.04 m3/s, the oil film on the water surface is disrupted due to high turbulence in the air bubble flow, and irregularities occur due to the oil film being dragged to the end of the test tank. These findings are consistent with the results of Lu et al. (2015).

Fig. 10 shows the absolute percentage error between numerical and experimental simulation. In gasoline, it was observed that as the air discharge from 0.01 $m^3$/s to 0.04 $m^3$/s absolute percentage error decreased from 12.68 % to 4.72 % in D = 1 mm, as the air discharge from 0.01 $m^3$/s to 0.04 $m^3$/s absolute percentage error decreases from 14.47 % to 2.73 % in D = 1.5 mm, as the air discharge from 0.01 $m^3$/s to 0.04 $m^3$/s absolute percentage error decreases from 18.6 % to 4.35 % in D = 2 mm. In diesel, it was observed that as the air discharge from 0.01 $m^3$/s to 0.04 $m^3$/s absolute percentage error decreases from 16.25 % to 10.08 % in D = 1 mm, as the air discharge from 0.01 $m^3$/s to 0.04 $m^3$/s absolute percentage error decreases from 14.12 % to 12 % in D = 1.5 mm, as the air discharge from 0.01 $m^3$/s to 0.04 $m^3$/s absolute percentage error decreases from 17.2 % to 12.21 % in D = 2 mm. In heavy fuel oil, as observed that as the air discharge from 0.01 $m^3$/s to 0.04 $m^3$/s absolute percentage error decreases from 18 % to 14.29 % in D = 1 mm, as the air discharge from 0.01 $m^3$/s to 0.04 $m^3$/s absolute percentage error decreases from 18.1 % to 13.85 % in D = 1.5 mm, as the air discharge from 0.01 $m^3$/s to 0.04 $m^3$/s absolute percentage error decreases from 23.48 % to 14.71 % in D = 2 mm.

As seen in Fig. 10, the absolute percentage error of heavy fuel is higher than the other 2 pollutants. This difference is believed to be a result of variations in the physical characteristics of the heavy fuel oil employed in the experimental setup compared to the heavy fuel oil employed in the numerical model. The lowest absolute percentage error has occurred in gasoline. This shows that the movement of gasoline on the water surface occurs close to what is modeled in the numerical simulation. Additionally, as the air volume flow rate increases, the absolute percentage error decreases especially in gasoline. It is thought that this is due to the limited length of the experimental setup.

Fig. 11 shows the mean absolute percentage error (MAPE) between numerical and experimental simulation. The average MAPE value for gasoline is 9.31 %. The average MAPE value for diesel is 13.23 % and the average MAPE value for heavy fuel is 17.06 %. These values meet the good forecasting in Table 3. When the two absolute percentage errors that are above 20 % for heavy fuel oil are removed, the average MAPE value for heavy fuel oil is 16.58 %. This inconsistency appears to be triggered by the following factors. The physical features of the fluids employed in the numerical model and experimental setup might be different. Numerical model and experimental setup dimensions might limit the studies. Since the tests were conducted in summer ambient conditions, the water and air temperatures may have affected the tests. In Fujita's (2016) study, it is seen that the correlation between the model and the experiment goes up to 20 %. MAPE values in this study are consistent with the results in Fujita (2016). Due to the complexity between water and air bubbles, it is recommended to change the turbulence model in the numerical simulation, repeat the analyses, and compare the results.

As previously explained, the core idea behind the ABB is to harness the reverse water flow generated by air to impede the natural water movement, thereby preventing the oil spill from extending further. The reverse water flow generated by the air substantially influences the ABB's effectiveness as an oil containment barrier. Air discharge is the primary factor that significantly affects air-driven reverse surface water flow. The larger the air discharge, the higher the effectiveness of the ABB in blocking marine pollution. However, it's important to observe that with the rise in air discharge, the rate at which the effective containment distance of the ABB increases decreases. Constantly providing high air discharge to the system to achieve a high effective containment distance may cause unnecessary energy consumption. The aperture diameter also affects the efficiency of the ABB in blocking marine pollution, although not as much as the air discharge. In addition, this study has shown that in the case of oil pollution, it is extremely significant which pollutant is

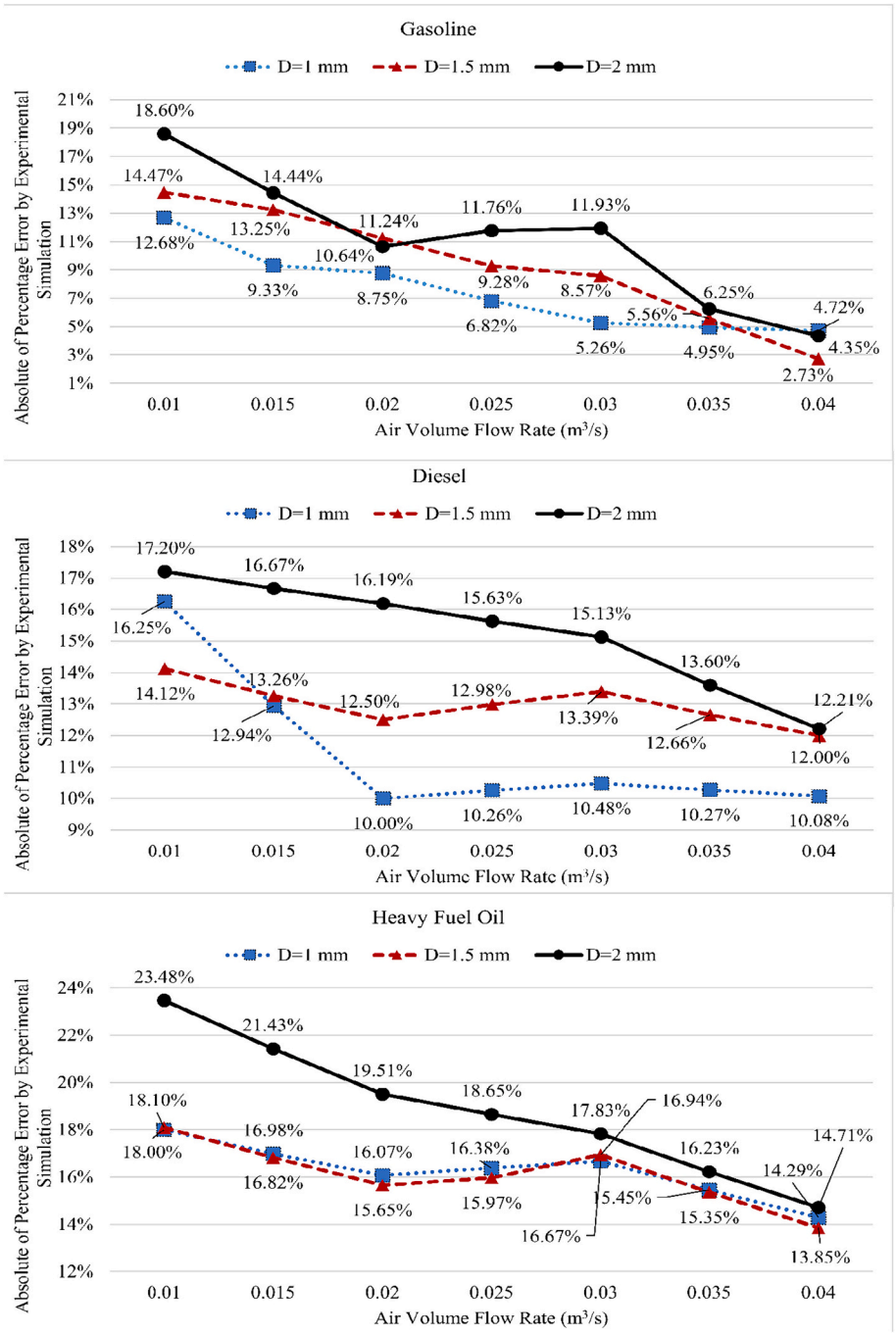


**Fig. 10.** Absolute percentage error between numerical and experimental simulation.

spilled into the sea. Response to marine pollution should be planned by considering the physical properties of the pollutant. For example, spilling a low-viscosity pollutant into the sea will require a higher air volume flow rate or aperture diameter to achieve the same effective containment distance as spilling a high-viscosity pollutant into the sea.

Based on current findings, this model is applicable for water intakes and port facilities, but additional studies may be necessary due to situations in the marine environment. The air feed pipe is positioned on a smooth bottom in the test tank, but improvements can be made to position the air feed pipe on the seabed. Since the tests have been performed with fresh water, seawater may trigger corrosion in the barrier materials. The experiments have been carried out in still water, but in the marine environment, additional tests should be carried out in case of bottom currents, bad weather, or wave conditions. It may be necessary to use additional pedestals to keep the air supply pipe stable on the seabed.

## 4. Conclusion

In this study, experimental and numerical simulations are conducted. The analysis of the ABB's impact on the effectiveness of preventing oil spill spreading is conducted by altering the aperture diameter, the air discharge, and the pollutant type. At the same time, the numerical and experimental simulations have been verified and validated using the MAPE score. It has been revealed that aperture diameter, air discharge, and pollutant type significantly affect the efficiency of the ABB on the spread of oil slick. The results of the present study show that air discharge affects the effectiveness of the ABB more than other

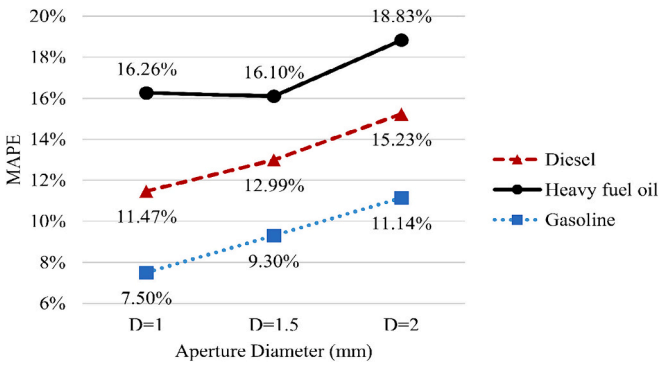


**Fig. 11.** Mean absolute percentage error (MAPE) between numerical and experimental simulation.

parameters. The findings of the study align with the results presented in the literature. This study differs from the literature in that it positions an adjustable air nozzle with a varying diameter on the air feed pipe and conducts experiments with different pollutants. This study has revealed that the feasibility of the suggested ABB as a tool for preventing the spread of oil spills is becoming increasingly promising. The results could provide valuable guidance for technical processes associated with the design and functioning of the ABB to contain marine pollution. This study will be helpful for companies and academics involved in the realm of oil spill response. At the same time, it is thought that this designed ABB can be applied to the breakwater mouths of terminals, ports, and marinas. After this study, an analysis of the ABB's impact on the efficiency of preventing oil spill spread will be conducted, with variations in aperture spacing, water depth, and air discharge considered. Additionally, full automation of the adjustable air nozzle and producing prototypes will be the focus of future work.

## CRediT authorship contribution statement

**Canberk HAZAR:** Writing – review & editing, Writing – original draft, Visualization, Validation, Software, Resources, Project administration, Methodology, Formal analysis, Data curation, Conceptualization. **Ali Cemal TÖZ:** Writing – review & editing, Supervision, Resources, Project administration, Methodology, Conceptualization.

## Declaration of competing interest

The authors declare the following financial interests/personal relationships which may be considered as potential competing interests: Ali Cemal Toz, Canberk Hazar has patent pending to Dokuz Eylul University. We have applied for a patent to our institution for this study. We are waiting to receive a patent application number from our institution. Therefore, if our article is accepted, we request that you set an embargo on the accepted paper until the patent application number is received. If there are other authors, they declare that they have no known competing financial interests or personal relationships that could have appeared to influence the work reported in this paper.

## Data availability

Data will be made available on request.

## Acknowledgments

This study derived from Canberk HAZAR's PhD thesis.

This work was supported by the Dokuz Eylul University Department of Scientific Research Projects (FDK-2021-2594). This study was supported by our institution with the patent application number 2024/000632, titled "Adjustable Pneumatic Barrier."

## Appendix A. Supplementary data

Supplementary data to this article can be found online at https://doi.org/10.1016/j.marpolbul.2024.116254.

## References

Abraham, G., Buirgh, P., 1964. Pneumatic reduction of salt intrusion through locks. Proc. Am. Soc. Civ. Eng. 90, 83–119.
Abraham, G., Van der Burg, P., De Vos, P., 1973. Pneumatic Barriers to Reduce Salt Intrusion through Locks. RWS-Communications. Vol. 17. Rijkswaterstaat, The Hague, Netherlands.
Bamdadinejad, M., Ketabdari, M.J., Rezaei, S., 2020. Pneumatic breakwaters and their use for ships protection in coastal and offshore areas of the Persian Gulf. J. Ocean Mech. Aerosp. Scie. Eng. 64 (3), 94–99. https://doi.org/10.36842/jomase.v64i3.219.
Basco, D.R., 1971. Pneumatic barriers for oil containment under wind, wave, and current conditions. In: Proceedings, Joint Conference on Prevention and Control of Oil Spills, American Petroleum Institute (API), June, Washington, DC, pp. 381–391.
Chen, J., Zhang, W., Wan, Z., Li, S., Huang, T., Fei, Y., 2019. Oil spills from global tankers: status review and future governance. J. Clean. Prod. 227, 20–32. https://doi.org/10.1016/j.jclepro.2019.04.020.
Cheng, Y., Zhao, N., Zhang, K., Wei, W., 2021. Research on the plume stability of air bubble curtains under low transverse flow velocity environment in dredging engineering. Ocean Eng. 232 (7), 109133 https://doi.org/10.1016/j.oceaneng.2021.109133.
Cui, P., Zhang, A.M., Wang, S.P., 2021. Shock wave emission and ice breaking effect of multiple interacting bubbles. Ocean Eng. 234 (6), 109175 https://doi.org/10.1016/j.oceaneng.2021.109175.
Delvigne, D.A.L., 1984. Laboratory Experiments on Oil Spill Protection of a Water Intake. Delft Hydraulics Laboratory, Publication No. 328, Delft, Netherlands.
Ditmars, J.D., Cederwall, K., 1974. Analysis of air bubble plumes. Coast. Eng. Proc. 1 (14), 128.
Eidnes, G., Leirvik, F., McClimans, T.A., Gjosund, S.H., Grimaldo, E., 2013. Containing Oil Spills by use of Air Bubbles. The International Society of Offshore and Polar Engineers (ISOPE).
Exair, 2023. Adjustable air nozzle. https://www.exair.com/adj.html.
Feng, Z., Zhang, B., 2023. Applications of bubble curtains in marine oil spill containment: hydrodynamic characteristics, applications, and future perspectives. Mar. Pollut. Bull. 194, 115371 https://doi.org/10.1016/j.marpolbul.2023.115371.
Fischer, H.B., List, E.J., Koh, R.C.Y., Imberger, J., Brooks, N.H., 1979. Mixing in Inland and Coastal Waters. Academic Press, New York.
Flammang, M.K., Weber, M.J., Thul, M.D., 2014. Laboratory evaluation of a bioacoustic bubble strobe light barrier for reducing Walleye escapement. N. Am. J. Fish Manag. 34, 1047–1054. https://doi.org/10.1080/02755947.2014.943864.
Fujita, I., 2016. Bubble Curtain for Blocking Spilled Oil on Water Surface. 2016 Techno-Ocean, pp. 354–359. https://doi.org/10.1109/Techno-Ocean.2016.7890678.
Gardiner, J., 2022. Finite element analysis convergence and mesh independence. https://www.xceed-eng.com/finite-element-analysis-convergence-and-mesh-independence/.
Grace, J., Sowyrda, A., 1970. The development and evaluation of a pneumatic barrier for restraining surface oils in a river. J. Water Pollut. Control Fed. Washington, DC 42, 2074–2093.
Haberlin, D., McAllen, R., Doyle, T.K., 2021. Field and flume tank experiments investigating the efficiency of a bubble curtain to keep harmful jellyfish out of finfish pens. Aquaculture 531, 735915. https://doi.org/10.1016/j.aquaculture.2020.735915.
Handå, A., McClimans, T.A., Reitan, K.I., Knutsen, O., Tangen, K., Olsen, Y., 2013. Artificial upwelling to stimulate growth of non-toxic algae in a habitat for mussel farming. Aquacult. Res. 45 (11), 1798–1809. https://doi.org/10.1111/are.12127.
Hazar, C., Töz, A.C., 2022. Use of air bubble barrier for oil containment: a literature review. In: 2nd Global Conference on Engineering Research (GLOBCER'22) Proceedings Book, pp. 126–133.
Hazar, C., Töz, A.C., 2023a. A mesh convergence study on 2-D air bubble barrier simulation with mean of inlet static pressure and horizontal surface velocity. Turk. J. Marit. Mar. Sci. 9 (1), 43–53. https://doi.org/10.52998/trjmms.1268375.
Hazar, C., Töz, A.C., 2023b. A comparative analysis of oil spill containment booms by means of operational efficiency for oil spill response. In: 1st International Maritime and Logistics Conference (MARLOGCONGRESS'23) Proceedings Book, pp. 180–190.
Hydrotechnik Lubeck, 2011. The advantage of pneumatic oil barriers. https://wpassets.porttechnology.org/wp-content/uploads/2019/05/25184457/PT32-27.pdf.
Ince, D., 1964. A guide to the design of air bubblers for melting ice. In: In Proceedings of the 9th Conference on Coastal Engineering, pp. 600–610.
ITOPF, 2022. Oil Tanker Spill Statistics 2022. ITOPF Ltd., London, UK.
Jones, W.T., 1972. Air barriers as oil-spill containment devices. Soc. Pet. Eng. J. 12, 126–142.
Kim, D.Y., Ha, J.Y., Paik, K.J., 2020. Numerical study on the extrapolation method for predicting the full-scale resistance of a ship with an air lubrication system. J. Ocean Eng. Technol. 34 (6), 387–393. https://doi.org/10.26748/KSOE.2020.008.
Kim, H.T., Kim, H.T., Kim, H.J., Kim, J.J., 2021. Study on the evaluation of frictional drag reduction by air lubrication and the arrangement of air injection parts for a liquefied natural gas carrier. J. Soc. Naval Architects Korea 58 (3), 144–157. https://doi.org/10.3744/SNAK.2021.58.3.144.

Kobus, H.E., 1975. On the use of air-bubble screens as oil barriers. In: International Association for Hydraulic Research, pp. 356–363.
Lau, Y.L., Engel, P., 1980. Control of oil slicks in flowing water using air-bubble barriers. Can. J. Civ. Eng. 7, 397–405.
Leander, J., Klaminder, J., Hellström, G., Jonsson, M., 2021. Bubble barriers to guide downstream migrating Atlantic salmon (Salmo salar): an evaluation using acoustic telemetry. Ecol. Environ. 160, 106141 https://doi.org/10.1016/j.ecoleng.2020.106141.
Lo, J.M., 1997. The effect of air-bubble barriers in containing oil-slick movement. Ocean Eng. 24 (7), 645–663.
Lu, J., Xu, Z., Xu, S., Xie, S., Wu, H., Yang, Z., Liu, X., 2015. Experimental and numerical investigations on reliability of air barrier on oil containment in flowing water. Mar. Pollut. Bull. 95, 200–206. https://doi.org/10.1016/j.marpolbul.2015.04.020.
Lube, G., Breard, E.C.P., Jones, J., Fullard, L., Dufek, J., Cronin, S.J., Wang, T., 2019. Generation of air lubrication within pyroclastic density currents. Nat. Geosci. 12 (5), 381–386. https://doi.org/10.1038/s41561-019-0338-2.
Lucke, K., Lepper, P.A., Blanchet, M.A., Siebert, U., 2011. The use of an air bubble curtain to reduce the received sound levels for harbor porpoises (Phocoena Phocoena). J. Acoust. Soc. Am. 130 (5), 3406–3412. https://doi.org/10.1121/1.3626123.
McClimans, T., Leifer, I., Gjøsund, S.V., Grimaldo, E., Daling, P., Leirvik, F., 2012. Pneumatic oil barriers: the promise of area bubble plumes. J. Eng. Marit. Environ. 0 (0), 1–17. https://doi.org/10.1177/1475090212450273.
Moreno, J.J., Pol, A.P., Abad, A.S., Blasco, B.C., 2013. Using the R-MAPE index as a resistant measure of forecast accuracy. Psicothema 25 (4), 500–506. https://doi.org/10.7334/psicothema2013.23.
Park, S.H., Lee, I., 2018. Optimization of drag reduction effect of air lubrication for a tanker model. Int. J. Naval Archit. Ocean Eng. 10 (4), 427–438. https://doi.org/10.1016/j.ijnaoe.2017.09.003.
Simmons, H.B., 1967. Potential benefits of pneumatic barriers in estuaries. Proc. Ame. Soc. Civil Eng. 93, 1–16.
Talimi, V., Thodi, P., Abdi, M.A., Burton, R., Liu, L., Bruce, J., 2020. Enhancing harsh environment oil spill recovery using air floatation system. Saf. Extreme Environ. 2, 57–67. https://doi.org/10.1007/s42797-019-00005-6.
Tsouvalas, A., Metrikine, A.V., 2016. Noise reduction by the application of an air-bubble curtain in offshore pile driving. J. Sound Vib. 371, 150–170. https://doi.org/10.1016/j.jsv.2016.02.025.
Wang, Y., Yin, Z., Liu, Y., Yu, N., Zou, W., 2019. Numerical investigation on combined wave damping effect of pneumatic breakwater and submerged breakwater. Int. J. Naval Archit. Ocean Eng. 11, 314–328. https://doi.org/10.1016/j.ijnaoe.2018.06.006.
Welton, J., Beaumont, W., Clarke, R., 2002. The efficiency of air, sound, and acoustic bubble screens in deflecting Atlantic salmon, Salmo salar L., smolts in the River Frome, UK. Fish. Manag. Ecol. 9, 11–18. https://doi.org/10.1046/j.1365-2400.2002.00252.x.
Wikipedia, 2023. Mean absolute percentage error. https://en.wikipedia.org/wiki/Mean_absolute_percentage_error.
Xu, T.J., Wang, X.R., Guo, W.J., Dong, G.H., Bi, C.W., 2019. Numerical simulation of the hydrodynamic behavior of a pneumatic breakwater. Ocean Eng. 180, 108–118. https://doi.org/10.1016/j.oceaneng.2019.04.010.
Zang, C., 2013. Numerical Simulation Study on the Submerged Pipe Depth of Air Bubbles Breakwater. Appl. Mech. Mater. 353-356, 2732–2735. https://doi.org/10.4028/www.scientific.net/AMM.353-356.2732.
Zang, C., Bai, L., 2012. Numerical Simulation Study on the Air Amount Scale of Air Bubbles Breakwater. Appl. Mech. Mater. 170-173, 2298–2302. https://doi.org/10.4028/www.scientific.net/AMM.170-173.2298.
Zdrazil, T., 2022. What are the disadvantages of booms for oil spills? https://www.absorbentsonline.com/spill-containment-blog/what-are-the-disadvantages-of-booms-for-oil-spills/.
Zielinski, D., Sorensen, P.W., 2016. Bubble curtain deflection screen diverts the movement of both Asian and common carp. North Am. J. Fish. Manag. 36, 267–276. https://doi.org/10.1080/02755947.2015.1120834.
Zielinski, D.P., Voller, V.R., Svendsen, J.C., Hondzo, M., Mensinger, A.F., Sorensen, P., 2014. Laboratory experiments demonstrate that bubble curtains can effectively inhibit movement of common carp. Ecol. Eng. 67, 95–103. https://doi.org/10.1016/j.ecoleng.2014.03.003.